

bradscholars

A mussel-inspired antibacterial hydrogel with high cell affinity, toughness, self-healing, and recycling properties for wound healing

Item Type	Article
Authors	Deng, X.;Huang, B.;Wang, Q.;Wu, W.;Coates, Philip;Sefat, Farshid;Lu, C.;Zhang, W.;Zhang, X.
Citation	Deng X, Huang B, Wang Q et al (2021) Mussel-inspired antibacterial hydrogel with high cell affinity, toughness, self-healing and recycling properties for wound healing. ACS Sustainable Chemistry and Engineering. 9(8): 3070-3082.
DOI	https://doi.org/10.1021/acssuschemeng.0c06672
Publisher	ACS PUBLICATION
Rights	© 2020 ACS. This document is the Accepted Manuscript version of a Published Work that appeared in final form in ACS Sustainable Chemistry and Engineering, copyright © American Chemical Society after peer review and technical editing by the publisher. To access the final edited and published work see https://doi.org/10.1021/acssuschemeng.0c06672 .
Download date	2026-04-19 02:18:13
Link to Item	https://bradscholars.brad.ac.uk/handle/10454/18387.2

A Mussel-Inspired Antibacterial Hydrogel with High Cell Affinity, Toughness, Self-Healing and Recycling Properties for Wound Healing

Xueyong Deng, ^{a, ‡} Bingxue Huang, ^{a, ‡} Qunhao Wang, ^a Wanlin Wu, ^a Phil Coates, ^c Farshid Sefat, ^{c,d} Canhui Lu, ^{a,e} Wei Zhang, ^{,a,e} Ximu Zhang, ^{*,b}*

a. State Key Laboratory of Polymer Materials Engineering, Polymer Research Institute at Sichuan University, Chengdu 610065, China.

b. Chongqing Key Laboratory of Oral Disease and Biomedical Sciences and Chongqing Municipal Key Laboratory of Oral Biomedical Engineering of Higher Education and Stomatological Hospital of Chongqing Medical University, Chongqing 401174, China

c. Interdisciplinary Research Centre in Polymer Science & Technology (Polymer IRC), University of Bradford, Bradford, UK.

d. Biomedical and Electronics Engineering Department, School of Engineering, University of Bradford, Bradford, UK.

e. Advanced Polymer Materials Research Center of Sichuan University, Shishi 362700, China.

Corresponding Author

*E-mail: weizhang@scu.edu.cn (W. Zhang).

*E-mail: zhangximu@hospital.cqmu.edu.cn (X. Zhang).

ABSTRACT: Antibacterial hydrogel has been intensively studied due to their wide practical potential in wound healing. However, developing an antibacterial hydrogel that able to integrate with exceptional mechanical properties, cell affinity and adhesiveness will remain a main challenge. Herein, a novel hydrogel with antibacterial and superior biocompatibility properties was developed using aluminum ions (Al^{3+}) and alginate-dopamine (Alg-DA) chains to crosslink with the copolymer chains of acrylamide and acrylic acid (PAM) via triple dynamic non-covalent interactions including coordination, electrostatic interaction and hydrogen bonding. The cationized nanofibrillated cellulose (CATNFC), which was synthesized by the grafting of long-chain quaternary ammonium salts onto nanofibrillated cellulose (NFC), was utilized innovatively in the preparation of antibacterial hydrogels. Meanwhile, alginate-modified dopamine (Alg-DA) was prepared from dopamine (DA) and alginate. Within hydrogel, the catechol groups of Alg-DA provided a decent fibroblast cell adhesion to the hydrogel. Additionally, the multitype cross-linking structure within the hydrogel rendered the outstanding mechanical properties, self-healing ability and recycling in pollution-free ways. The antibacterial test in vitro, cell affinity and wound healing proved that the as-prepared hydrogel was a potential material with all-rounded performances in both preventing bacterial infection and promoting tissue regeneration during wound healing processes.

KEYWORDS: Antibacterial hydrogel, Cationized nanofibrillated cellulose (CATNFC), Alginate-dopamine (Alg-DA), Self-healing, Wound-healing.

INTRODUCTION

Skin tissue is one of the most important parts of human body. It plays an irreplaceable role in maintaining the body's environmental balance and protecting the body from a variety of harmful substances.^{1,2} It has massive surface area and is usually exposed to the environment, making it a very vulnerable tissue in human body.^{1,2} Under severe skin infections, the wound can cause serious consequences that impact the health and life of people. Infection within skin usually results in extended wound healing and implantation failure which eventually end up with more complicated problems within human body, even mortality. However, it is worried that the healing processes of wounds are time-consuming, especially for the extensive full-thickness wounds.³ One of the major challenges with national health services round the world is to repair acute and chronic wounds as quick as possible. Therefore, new materials with all-rounded properties in preventing bacterial infections, promoting healing progresses and suppressing scar formations are urgently demanded.⁴ In recent years, various types of wound dressings such as electrospun nanofibers,⁵ foams,⁶ membranes,⁷ and hydrogels⁸ are intensively studied. Among these materials, the hydrogel dressing has attracted considerable research interests due to its advantages in wound moisture maintaining, exudate absorption and surface cooling, resulting in pain-relief.⁹ Compared to regular hydrogels, those with antibacterial characteristics are capable of fighting with bacterial infectious diseases.¹⁰ For most antibacterial hydrogels, antibiotics are usually incorporated to prevent bacterial infection. But the antibiotic overuse potentially results in drug resistance of bacteria. Moreover, some antibacterial hydrogels combined with bactericides have been reported. Silver nanoparticles are widely added in hydrogels as antibacterial particles, which have the disadvantages of being expensive as well as high biotoxicity.¹¹ Therefore, it is urgent to find a cheap and biocompatible bactericidal agent. The use of antibacterial materials, such as cationic polymers, offers a possible strategy in the development of antimicrobial hydrogels. In particular, the quaternary

ammonium polymers exhibit good antibacterial capabilities, which is related to the existence of abundant cations on the molecular chains.^{12,13} Natural polymers, such as cellulose, have been widely utilized in biomedical applications, due to their significant biocompatibility and mechanical properties.¹⁴ However, cellulose has no antibacterial properties in nature and is not easily dispersed. In recent years, some researchers have prepared antibacterial nanofibrillated cellulose (NFC) by cationization.¹⁵ Nonetheless, due to the antibacterial mechanism of quaternary ammonium compounds (QACs), the prepared antibacterial cellulose did not demonstrate strong antibacterial effect on gram-negative bacteria represented by *E. coli*.¹⁶ According to current research, the performance of QACs-based antimicrobial materials can be profoundly impacted by the molecular weight of the QAC.¹⁷ Also, the N-alkyl chain length has impact on the antimicrobial activities of QACs. The longer the N-alkyl chain, the stronger the antimicrobial capability.¹⁸ It provides new possibilities for the fabrication of hydrogel materials possessing good antibacterial activities and prolonged efficacies without the use of toxin and antibiotic drugs.

Other than the antibacterial property, adequate mechanical properties, such as toughness and recoverability are the essential requirements for hydrogels in their application in wound healing. Hydrogels with unsatisfied mechanic characters are not a good candidate for wound healing.¹⁹ For decades, several strategies, such as double-networks (DN),²⁰ nanocomposites,⁷ and ionic crosslinking,²¹ are applied to improve the mechanical properties of hydrogels. Among them, DN are the typically used form of tough hydrogels based on the energy dissipation mechanism.^{22,23} As reported by Wang et al.,²⁴ poly (acrylic acid) and chitosan were used to develop DN hydrogels via metal-coordination and chain entanglement. And the hydrogels demonstrated fine anti-fatigue and self-healing performances due to their supramolecular structure. Furthermore, there is no doubt that hydrogel dressings capable of rapid self-healing can restore the lesion and therefore have longer duration of usage.^{25,26} In a latest study,

hydrogels integrating over 2 types of physical or chemical interactions in a single system are often associating with better mechanical properties and excellent self-healing abilities.²⁷ This should be attributed to the synergistic actions of the efficient energy dissipation mechanism and the results of dynamic chemical covalent bonds.²⁸ Nonetheless, most of these tough hydrogels are not suitable for cell growth and have poor bio-adhesion, thereby limiting their applications in wound healing. Recently, catechol chemistry enlightens the preparation of materials with cell adhesive and affinitive properties, due to its molecular structure alike to the adhesive proteins extracted from mussels.²⁹⁻³¹ The hydrogels incorporated with polydopamine (PDA) are typical adhesive materials based on catechol chemistry.³²⁻³⁴ The PDA hydrogel contains catechol functional groups, which construct covalent or noncovalent bonds with different surfaces, leading to improved adhesive properties to cell and tissue.³⁵ Besides, the catechol functional groups in hydrogels produce improvements in both adhesive and cohesive properties under wet conditions. Furthermore, PDA is increasingly applied in the development of antibacterial hydrogels supporting the growth of cell. For example, Gan and co-workers reported an antibacterial hydrogel with remarkable cell affinity, which was synthesized from methacrylamide dopamine and 2-(dimethylamino) ethyl methacrylate copolymerizations.³⁶ Therefore, the incorporation of dopamine as well as its derivatives is potentially practicable in improving the properties of hydrogels, including tissue affinity and adhesion.

In this research, a novel antibacterial hydrogel without cytotoxicity was prepared using Al^{3+} and alginate-modified dopamine (Alg-DA) chains to crosslink with the acrylamide and acrylic acid copolymer (PAM) chains via triple dynamic non-covalent interactions, including coordination, hydrogen bonding and electrostatic interaction. This hydrogel possessed several improvements listed as follow. First, unlike the antibacterial hydrogels using antibiotic components, the new hydrogel showed inherently contact-active antibacterial activities. NFC grafted with long-chain QACs was innovatively utilized in antibacterial hydrogel preparation.

Another advantage is that the cationized nanofibrillated cellulose (CATNFC) itself is mechanically strong, which can serve as an effective reinforcing filler for the hydrogel. Benefited from the triple-crosslinked network together with the dynamic non-covalent bonds, the as-prepared Alg-DA-CATNFC-PAM- Al^{3+} DN hydrogel exhibited desirable mechanical performance and self-healing property. Besides, it could also be easily recycled in pollution-free ways. Moreover, compared with other tough and antibacterial hydrogels that were typically not favorable for cell growth, this hydrogel exhibited significant improvement in cell and tissue affinities through the presence of Alg-DA. Hence, it held high potential in the applications of repairing soft tissue lesions and preventing bacterial infections of the wounds.

RESULTS AND DISCUSSION

The Design rationale of hydrogel

The materials with excellent antibacterial property, good adhesiveness and biocompatibility are conducive to providing a desirable environment for wound healing. In order to shorten the time of wound healing, a multi-physically-cross-linked DN hydrogel, namely, Alg-DA-CATNFC-PAM- Al^{3+} DN hydrogel, was prepared in two steps (Figure 1b). First, the synthesized Alg-DA, CATNFC, acrylamide and acrylic acid (5mol% of acrylamide) were polymerized with ammonium persulfate (APS) as the initiator to form the Alg-DA-CATNFC-PAM hydrogels. In these hydrogels, CATNFC with excellent antibacterial ability was obtained by grafting 12-carbon QACs onto NFC (Figure 1a). In addition to hydrogen bonding interactions, the charged cations on CATNFC could form electrostatic interactions with the carboxyl anions to further improve the mechanical properties of hydrogels. Alginate has been extensively used for adipose tissue regeneration, wound dressing and in general for soft tissue engineering, due to its excellent biocompatibility and safe gelation.^{37,38} However, it is worth to note that because of the limited cell adhesion sites, alginate has poor cell adhesion.³⁹ Inspired by mussels, Alg-DA was prepared from dopamine and alginate (Figure S1), which exhibited

enhanced cell adhesion owing to the introduction of the catechol moieties.⁴⁰ In the second step, the Alg-DA-CATNFC-PAM hydrogel was immersed in the Al^{3+} solution. Notably, metal ions have been widely used in the preparation of hydrogel wound dressings.⁴¹⁻⁴³ Compared with other metal ions, Al^{3+} is much attractive owing to its excellent antibacterial property and low cytotoxicity.^{44,45} The metal-ligand coordination crosslinking between Al^{3+} and Alg-DA was constructed using the catechol group of DA as the crosslinking point. As a result, the hydrogel formed a DN structure, leading to enhanced mechanical strength. In addition, the as-prepared Alg-DA-CATNFC-PAM- Al^{3+} DN hydrogels exhibited outstanding self-healing abilities after damage, which should be ascribed to the metal-ligand coordination.

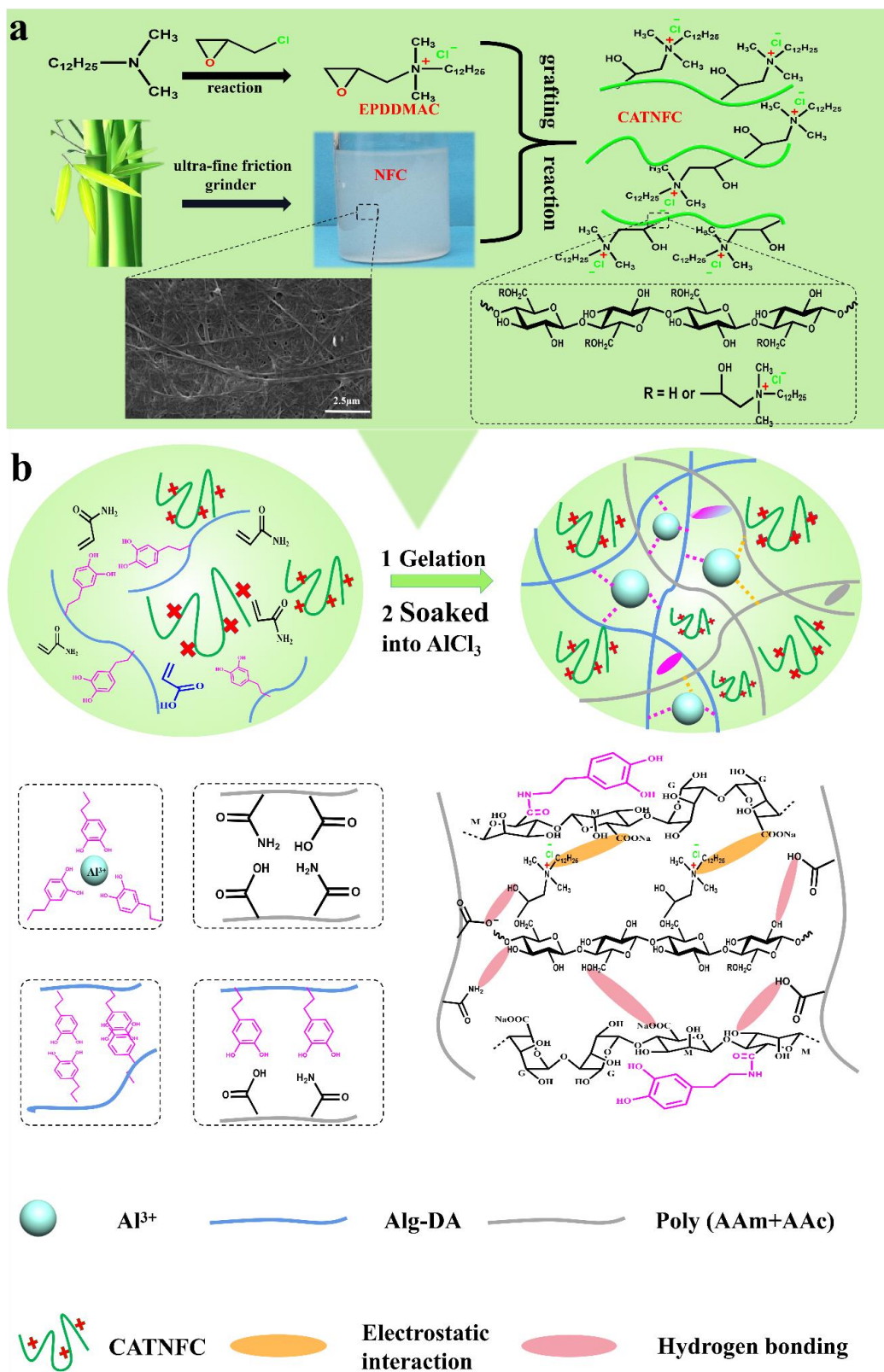


Figure 1. The design rationale of the hydrogel (a) The preparation principle of CATNFC (b) The structure of the hydrogel and the multiple interactions at the molecular level.

The Fourier transform infrared (FTIR) spectra in Figure S2 coupled with the proton nuclear magnetic resonance (^1H NMR) spectra in Figure S3 verified that the epoxypropyl dodecyl dimethyl ammonium chloride (EPDDMAC, see the discussion in Supporting Information) was successfully prepared. NFC and CATNFC were analyzed by FTIR spectroscopy (Figure S4). The neat NFC displayed several bands at 3332 cm^{-1} , 2900 cm^{-1} and 1103 cm^{-1} which were due to the stretching of $-\text{OH}$, $\text{C}-\text{H}$ of $-\text{CH}_2-$ and $\text{C}-\text{O}$ from secondary alcohol, respectively. After cationization modification, new peaks were found at 2893 cm^{-1} and $1215\text{-}1280\text{ cm}^{-1}$, owing to the stretching of $\text{C}-\text{H}$ from $-\text{N}^+(\text{CH}_3)_2-$ and the stretching vibration of $\text{C}-\text{N}$, respectively. A sharp peak was obtained at 993 cm^{-1} , which was ascribed to the new $\text{C}-\text{O}-\text{C}$ formed by grafting quaternary ammonium. These results indicated the quaternary ammonium was successfully grafted onto the cellulose. In addition, the elemental composition of CATNFC was determined. Natural cellulose does not contain nitrogen element. However, the elemental analysis showed that a certain proportion of nitrogen existed in the product, which consistently proved the successful synthesis of CATNFC. Furthermore, the percentage of nitrogen was used to estimate the degree of substitution (DS) (Table S1). In order to verify if the as-prepared CATNFC could effectively kill gram-negative bacteria, antibacterial test against *E. coli* was conducted on NFC, EPTMAC-NFC ($DS=0.192$) and CATNFC ($DS=0.182$). The results (Figure S5) showed that CATNFC had the best antibacterial effect. Besides, the peaks appeared at $6.5\text{--}7.0\text{ ppm}$ in the ^1H NMR spectrum (Figure S6) confirmed that DA was successfully introduced to the alginate structure.⁴⁶ Moreover, the peak of UV absorption at 280 nm in Figure S7 further indicated the successful synthesis of Alg-DA.

The morphologies of hydrogels after freeze-drying were observed by a scanning electron microscope (SEM). As shown in Figure S8, compared with the smooth layer surface of Alg-DA-PAM- Al^{3+} hydrogel, the Alg-DA-CATNFC-PAM- Al^{3+} hydrogel displayed a state of nanofibers winding owing to the presence of CATNFC. The cationic groups and hydroxyl

groups in CATNFC provided a large number of active points, which could be cross-linked with the chains of Alg-DA and PAM through hydrogen bonding and electrostatic interaction (Figure 1b). To detect the distribution of Al^{3+} in hydrogels, an EDS mapping test was performed. According to the image analysis (Figure S9), the Al^{3+} ions were evenly distributed in the hydrogel.

Mechanical Properties

The hydrogel demonstrated promising mechanical behaviors, especially in recoverability. As shown in Figure 2e, the cylindrical hydrogel was capable of withstanding a compression strain of 80% without fracture. When the pressure was released, the cylindrical hydrogel recovered its original shape in five minutes. As a control, Alg-DA-PAM, Alg-DA-PAM- Al^{3+} and Alg-DA-CATNFC-PAM hydrogels were also prepared. As shown in Figure 2b, the stresses of the four different hydrogels at 60% compressive strain were 83.13 KPa, 307.97 KPa, 120.78 KPa and 385.09 KPa, respectively. Moreover, the curves in Figure 2a indicated that the compressive stress of the DN hydrogel was much higher than that of the single network hydrogel under the same strain. Specifically, when the compressive strain reached 60%, the compressive stress of the DN hydrogel was more than three times that of the single network hydrogel. These results implied that the mechanical properties and stability of the DN hydrogel were significantly improved owing to the multiple interaction mediated network, which was constructed via reversible non-covalent interactions, such as coordination, hydrogen bonding and electrostatic interactions. Additionally, CATNFC could also effectively enhance the compression performance of the hydrogel. According to the data, the addition of CATNFC increased the compressive stress by more than 30% under 60% compressive strain. This phenomenon should be ascribed to the two reasons. Firstly, CATNFC acted as a filler to reinforce the polymer hydrogels owing to its excellent mechanical properties. Secondly, the stability of hydrogels under stress was improved with CATNFC as it provided more crosslink

points to increase the crosslinking density of the network. To further investigate the influence of crosslinking density on the mechanical performance of hydrogels, Alg-DA-CATNFC-PAM single network hydrogels were immersed in Al^{3+} solutions with various ion concentrations to prepare DN hydrogels with different crosslinking densities. As the ion concentration increased, the compressive stress increased remarkably (Figure 2c, d). However, further increase in the mechanical strength was not obvious when the ion concentration was higher than 0.11 M, suggesting a saturated crosslinking state was reached. These results indicated that the increase of cross-linking points could make the DN structure more stable and the mechanical properties of the hydrogel further improved.

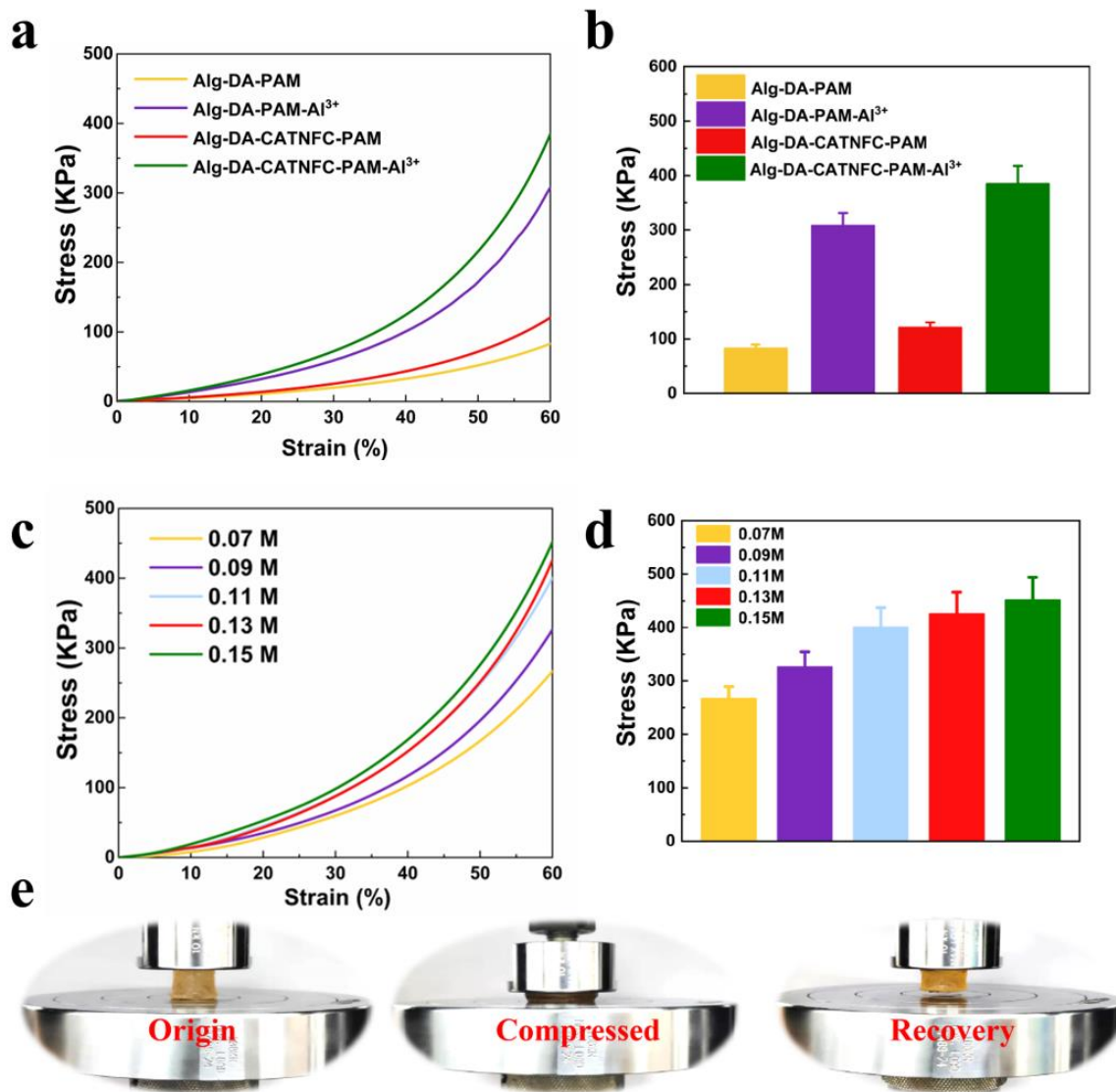


Figure 2. The mechanical properties of different hydrogels. (a) Typical compressive stress–strain curves for various types of hydrogels. (b) Compression modulus of various types of hydrogels at the compressive strain of 60%. (c) Typical compressive stress–strain curves for hydrogels crosslinked with ion solutions of different concentrations. (d) Compression modulus of various types of hydrogels at the compressive strain of 60% (e) Images showing that the Alg-DA-CATNFC-PAM-Al³⁺ hydrogel could recover without breakage after compressed up to a strain of 80%.

Self-Healing and Recycling Properties

In addition to the improved mechanical properties, the Alg-DA-CATNFC-PAM- Al^{3+} DN hydrogel also showed unique self-healing and recycling properties. The hydrogels could self-heal without any agent owing to the dynamic interactions. As schemed in Figure 3a, the Al^{3+} on the fracture surface remained reactive to the Alg-DA chains via strong coordination interaction. Meanwhile, Al^{3+} gradually diffused toward the fracture interface with the help of the mobility of Alg-DA chains, which promoted the reconstruction of electrostatic interactions and coordination bonds.⁴⁷ Besides, the hydrogen bonds could also be rebuilt when the two separated parts came into contact.

In order to demonstrate the self-healing ability of the DN hydrogel, three differently colored cylinders of hydrogel were prepared. They were then attached to each other for self-healing at room temperature. The three hydrogels were combined into a bulk hydrogel after 12 h. The healed hydrogel from the three pieces was highly robust with strong interphase interaction at the healing sites. As a result, it could be bent or stretched, and easily lift a load of 500 g without breaking (Figure 3b). In addition, color diffusion was observed at the junction of the three hydrogel pieces, which vividly implied the segment migration and ion diffusion at the interphase. In order to detect the time-dependent self-healing process, the maximum tensile stresses for the original hydrogel and the hydrogels after self-healing for 8 and 24 h were evaluated. In Figure 3d, the maximum tensile stress of the original hydrogel was 128.76 KPa, while the value was 106.33 KPa after 8 h self-healing, and 118.24 KPa after 24 h self-healing. In other words, the maximum tensile stress of hydrogel retained 82.57% of the original value after 8 h self-healing and 91.83% after 24 h. Furthermore, the healing of the incision was observed on an ultra-depth microscope. As shown in Figure 3c, the cutting healed well after 8 h, and almost recovered the original state after 24 h. All the results consistently indicated that the DN hydrogel had outstanding self-healing capability and efficiency.

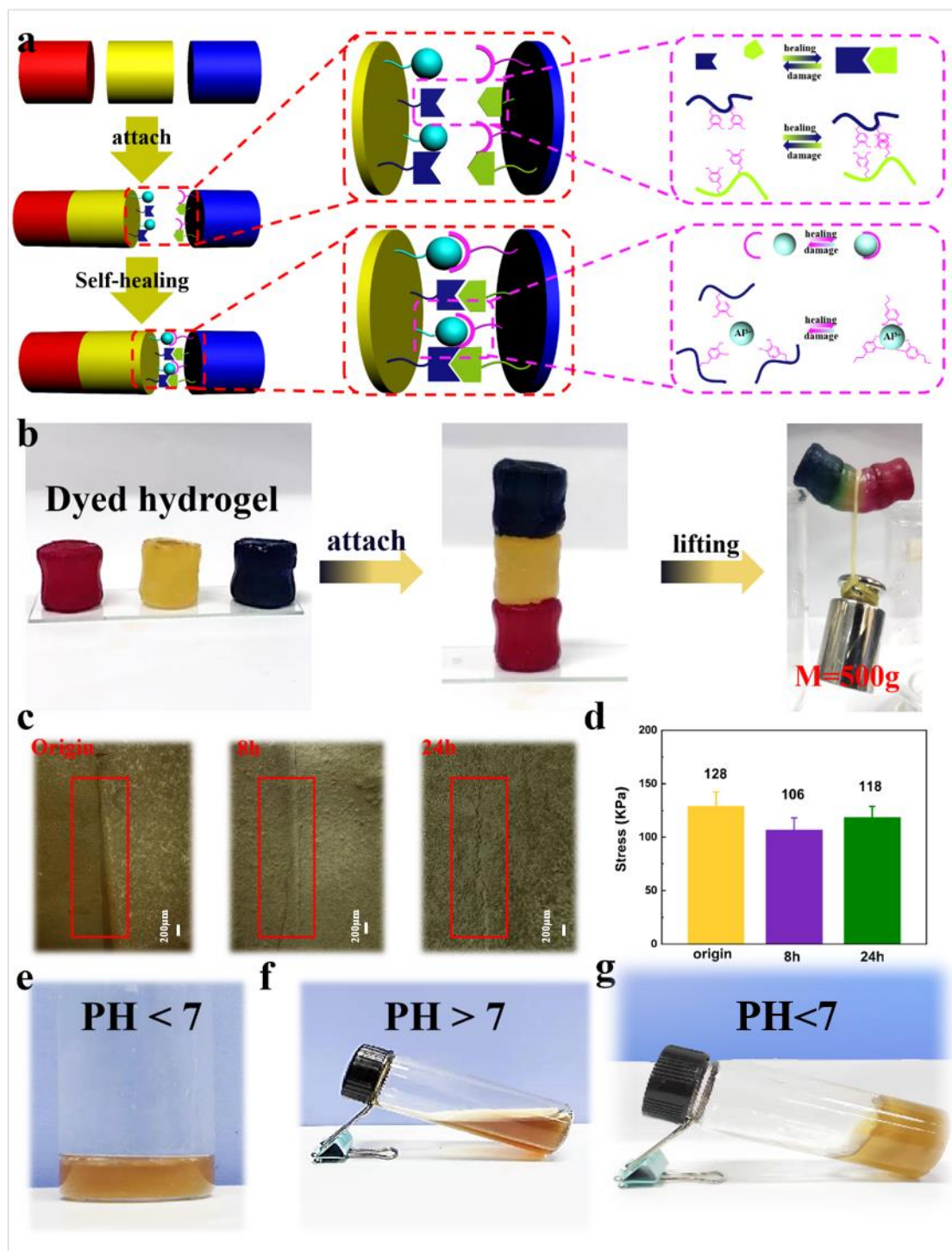


Figure 3. Self-healing and recycling properties of the Alg-DA-CATNFC-PAM- Al^{3+} hydrogel.

(a) Self-healing mechanism. (b) Self-healing validation experiment. (c) Images of damaged and healed samples observed on an ultra-depth microscope. (d) Maximum tensile modulus of original and self-healed hydrogels (8h, 24h). (e) Pre-recycle hydrogel. (f) The hydrogel after dropping lye. (g) The hydrogel recycled by adding acetic acid.

Another attractive finding was that the DN hydrogel could be recycled easily. Due to the dynamic physical crosslinking structure, Alg-DA-CATNFC-PAM- Al^{3+} DN hydrogel could be dissolved in 1 M sodium hydroxide solution without any damage to the PAM and Alg-DA chains (Figure 3f). As a consequence, the physical network of Alg-DA-CATNFC-PAM- Al^{3+} hydrogel could be rebuilt by adding acetic acid solution dropwise. When pH was high, the coordination between Al^{3+} and o-phenylenedihydroxy group would dissociate due to the reaction of Al^{3+} and OH^- ions to form $\text{Al}(\text{OH})_3$,⁴⁸ which resulted in the collapse of the hydrogel network. However, when adjusted the $\text{pH} < 7$ using the acetic acid solution, the metal coordination bond was restored and a hydrogel was formed again.⁴⁹ Since only acetic acid and sodium hydroxide were used in this conversion process, the recycled hydrogels should be safe and pollution-free.

Adhesiveness

The present hydrogel was discovered to have excellent adhesiveness to a variety of materials. As shown in Figure 4b, the hydrogel could adhere to the surfaces of polypropylene (PP), glass, Polytetrafluoroethylene (PTFE), and rubber. Additionally, it had outstanding adhesive performance to various tissues (kidney, liver, and muscle), which was critical for applications in biomedicine (Figure 4b). In particular, the hydrogel exhibited high adhesiveness on the surface of human skin. Notably, the hydrogel sticking to the skin would not induce anaphylactic reactions, and could be peeled off without leaving any residue. Moreover, owing to the excellent stretchability and compressive performance, when the hydrogel was applied on human joint skin, one could freely bend his/her knuckle, elbow and knee (the angle from 0° to 120°) without a feeling of any hindrance (Figure 4c), showing promise in joint skin wound dressing. In order to further simulate the application scenario in life, a motion adhesion model on rats was demonstrated. In this experiment, 8 pieces of hydrogels were dressed on 8 rats, respectively. After their free exercise for 12 h, 7 pieces of hydrogels were found still well

attached to the rat back. Furthermore, its adhesive strength on the surfaces of different tissues was quantified in a tensile adhesion test (Figure 4d). As shown in Figure 4e, the adhesive strength on fat and pig skin was 5.3 KPa and 15.3 KPa, respectively.

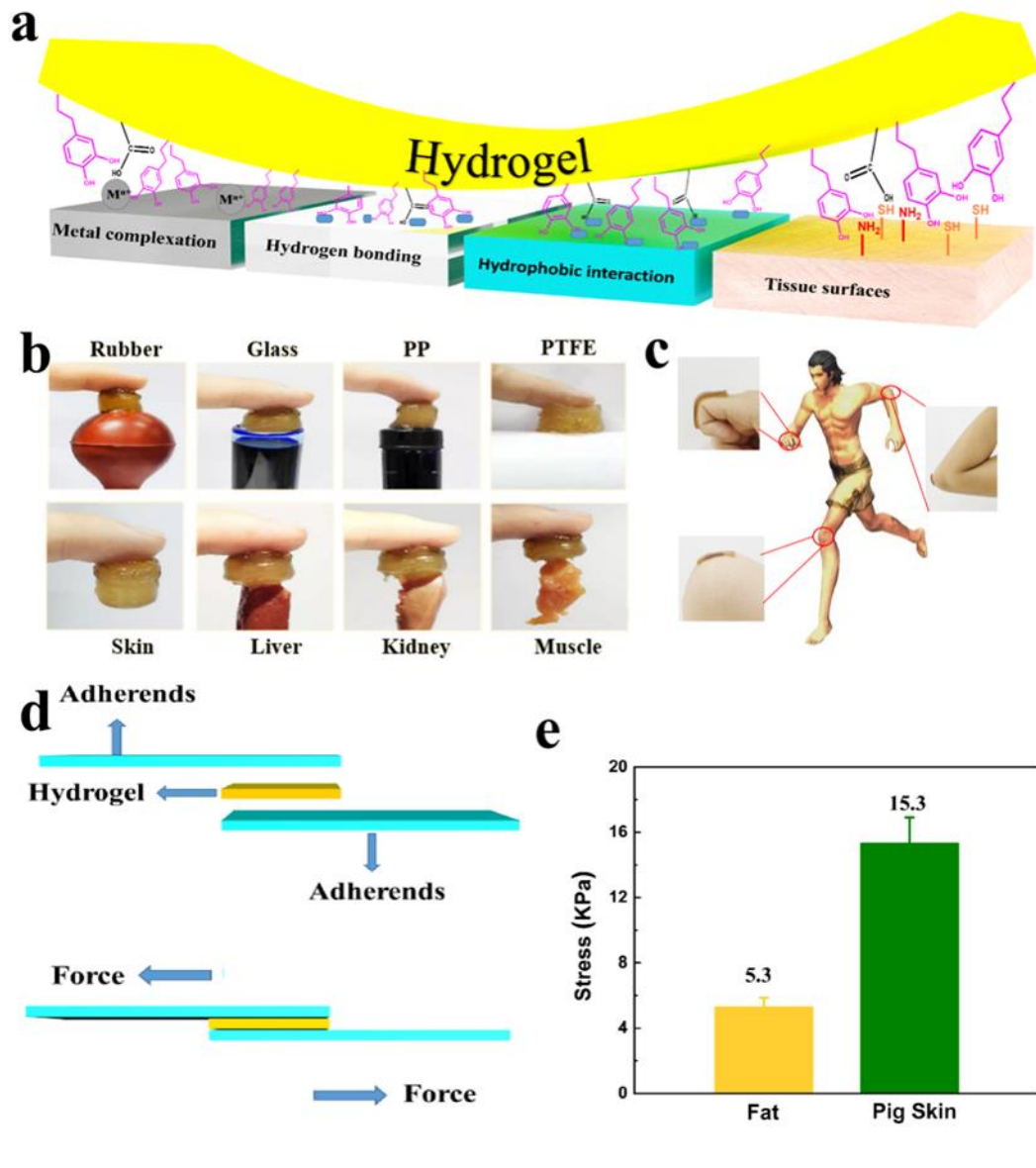


Figure 4. Adhesive performance of Alg-DA-CATNFC-PAM-Al³⁺ hydrogel. (a) The adhesion mechanism. (b) Attachment to various materials and tissues. (c) Attachment to various human body joints. (d) The model for testing adhesion properties. (e) The adhesive strength of the hydrogel on fat and pig skin.

The excellent adhesion of the hydrogel should be mainly ascribed to the presence of the catechol group of dopamine and the carboxyl group of alginate. Firstly, the carboxyl groups can interact with the surfaces of various substrates by electrostatic interactions. Secondly, the catechol groups of dopamine possess strong adhesion to various materials via noncovalent and covalent bonding (Figure 4a). Covalent bonding is established at some substrates with thiol or amine groups via Michael addition or Schiff base reactions. Additionally, there also exist noncovalent bonding (π - π stacking, hydrogen bonding, and metal chelating or coordination) between the hydrogel and the surface of material.⁵⁰

In Vitro Antibacterial Study

The present hydrogel demonstrated prominent antibacterial activity due to the synergistic influences of CATNFC, Alg-DA and Al^{3+} . As schemed in Figure 5e, the Alg-DA has excellent bio-adhesion properties, thus it can provide the hydrogel with stronger adhesion. This will facilitate the contact with bacteria at the wound site, and improve the antibacterial effectiveness of CATNFC. The antibacterial activities of this hydrogel were evaluated in the growth tests of *Staphylococcus aureus* (*S. aureus*, gram-positive organism), and *Escherichia coli* (*E. Coli*, gram-negative organism). The counter board pictures of respective bacterial growth on different hydrogels were presented in Figure 5a and b. The number of bacteria for Alg-DA-PAM- Al^{3+} hydrogel was lower as compared with those in control groups, because Al^{3+} had antibacterial effects. Besides, with the addition of CATNFC, the resultant hydrogel demonstrated much improved antibacterial properties. This result further confirmed that CATNFC was an excellent antibacterial additive for hydrogels. In addition, the suspension with Alg-DA-CATNFC-PAM- Al^{3+} hydrogel was the clearest, suggesting strong bactericidal activities. As revealed by the quantitative analysis, the *E. coli* bactericidal ratios of Alg-DA-PAM and Alg-DA-PAM- Al^{3+} hydrogels were 7% and 44%, respectively (Figure 5d). In comparison, Alg-DA-CATNFC-PAM and Alg-DA-CATNFC-PAM- Al^{3+} hydrogels

demonstrated significantly higher antibacterial ratios (94% and 97%, respectively). The bactericidal ratios of *S. aureus* for the hydrogels exhibited a similar trend. The bactericidal ratios of *S. aureus* for Alg-DA-CATNFC-PAM and Alg-DA-CATNFC-PAM- Al^{3+} hydrogels were 71.4% and 85.7%, respectively (Figure 5c). In summary, the Alg-DA-CATNFC-PAM- Al^{3+} hydrogel could effectively inhibit both gram-positive and gram-negative bacteria. The wide-spectrum antibacterial abilities of CATNFC endowed the hydrogel with excellent antibacterial properties, which were further improved by the activities of Al^{3+} .

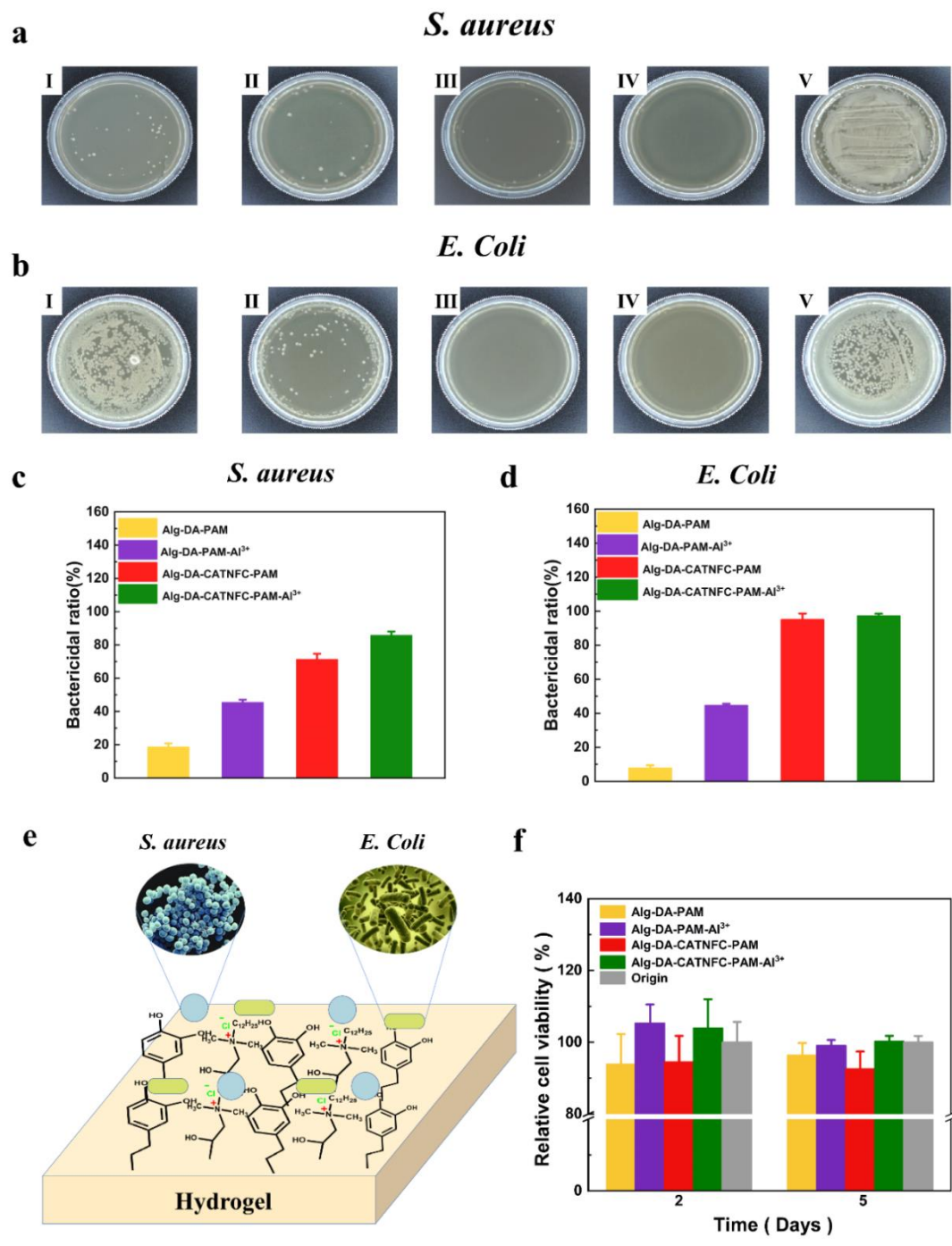


Figure 5. The antibacterial properties of the hydrogels. (a) Pictures of *S. aureus* suspensions co-cultured with the I) Alg-DA-PAM hydrogel, II) Alg-DA-PAM-Al³⁺ hydrogel, III) Alg-DA-CATNFC-PAM hydrogel, IV) Alg-DA-CATNFC-PAM-Al³⁺ hydrogel, V) control sample. (b) Photos of *E. Coli* suspensions co-cultured with the hydrogels. (c) Bactericidal ratios on *S. aureus*. (d) Bactericidal ratios on *E. Coli*. (e) Schematic of the antibacterial activity. (f) The proliferation of fibroblasts on different hydrogels.

In Vitro Cell Affinity

The superior cell affinity can promote cell growth. Fibroblasts are the typical cell type primarily involved in wound-healing.⁵¹ To test the cell affinity of the prepared hydrogels, fibroblasts were cultured on various hydrogels. From the optical micro-images in Figure S10, fibroblasts could be well cultivated on all hydrogel surfaces for 24 h, suggesting their non-cytotoxicity. Furthermore, the cell growth after 2 and 5 days culture on the hydrogels was quantitatively evaluated (Figure 5f). The fibroblasts maintained above 85% in relative cell viability for all the experiment groups after 2 days culture. The number of cells cultured on Alg-DA-CATNFC-PAM- Al^{3+} DN hydrogel was even higher than that on the natural culture. According to the literatures, Al^{3+} at low concentrations can promote the growth of human skin fibroblasts by affecting lipid peroxidation and DNA synthesis.^{52,53} After 5 days culture, the obtained data was similar to that for 2 days culture. These results indicated that the hydrogels had good cell affinity.

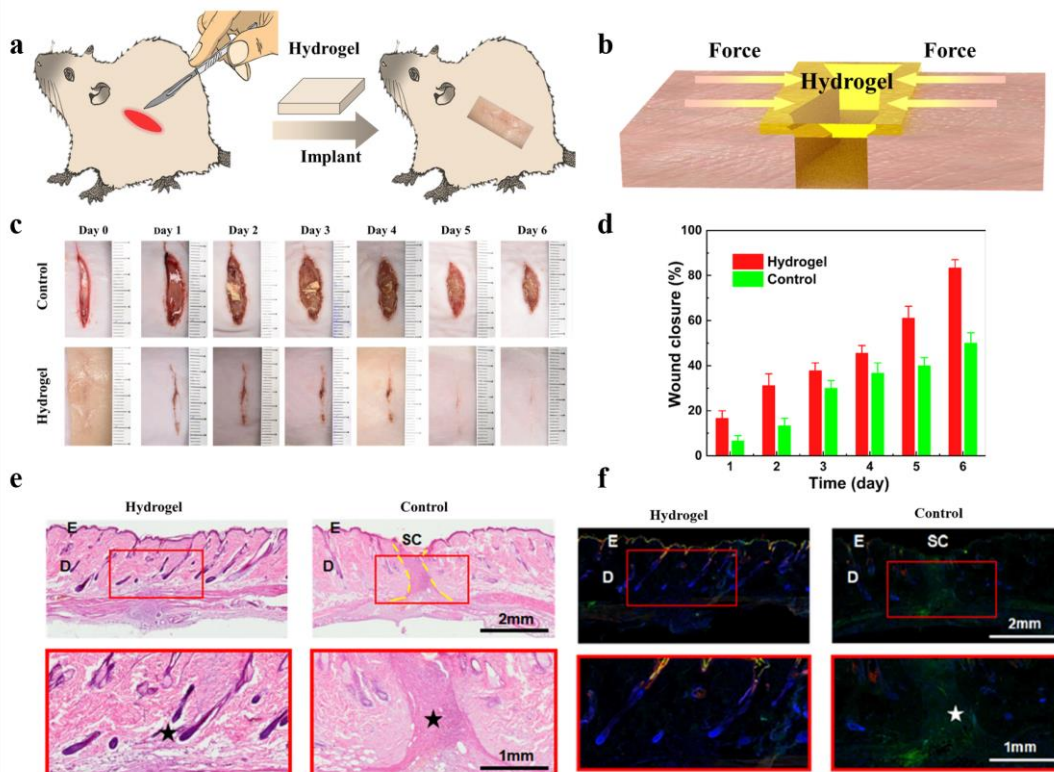


Figure 6. (a) Schematic of the hydrogel treatment on the wound site. (b) Schematic of the hydrogel suture. (c) Representative pictures showing the gross appearance of incisions after different periods. (d) Wound closure rate calculated from equation (1) for the wound treated with the hydrogel and the control. (e) Representative pictures of Hematoxylin-eosin (H&E) staining of the wound incision sites after 6 days of treatments. Epidermis (E), dermis (D), scab (SC), incision site (★), wound area (within yellow line) is indicated. (f) Representative pictures of immunofluorescence staining of CD3⁺ cells (lymphocytes) and CD68⁺ cells (macrophages) demonstrating inflammatory responses around incision sites after 6 days of treatments, while more serious inflammation appeared in the blank control group. CD3⁺ cell: Red; CD68⁺ cell: green; nuclei: blue. **p < 0.01, ***p < 0.001.

Healing Infected Skin Incision In Vivo

Skin incision model of rats was used for wound-healing assessments of hydrogels *in vivo*. In order to more realistically imitate the wound by sharp blade in daily life, a scalpel was used to cut a 30 mm opening on the back skin of the experimental rats and bacterial liquid was dripped into the opening (Figure 6a). By comparing the wound infection and wound healing in the control group, it could be determined whether the hydrogel could promote wound healing. As shown in Figure 6c and d, the rats in the control group had bacterial infection on the second day after injury. By contrast, the rats using the hydrogel wound dressing were not infected. This is because CATNFC in the hydrogel effectively killed bacteria on the wound site and prevented external bacteria from invading the wound (Figure 5e). Additionally, the wounds with the hydrogel did not show tearing and tissue nakedness as in the control group in the early stage of healing, which was believed to be due to the good biological adhesion of hydrogels. The excellent adhesive property of hydrogel allowed good closure of tissue opening of the wound, functioning like the surgical thread (Figure 6b). This could prevent the wound tissue from further tearing due to the strenuous exercise of rats.

At day 6 after the incision operations, histological analysis was performed for the evaluations of wound-healing processes and potential adverse effect in hydrogel treatments (Figure 6e). With the treatments of Alg-DA-CATNFC-PAM- Al^{3+} hydrogels, the incisions constantly healed from the basement membrane without severe opening at the incision sites. Moreover, at the incision sites treated with Alg-DA-CATNFC-PAM- Al^{3+} hydrogels, necrotic cells were presented sporadically with no nuclear (blue) staining found in the basal area. Meanwhile, incision sites treated with hemostasis demonstrated granulated tissue, characterized by scabbing and ulcerous appearances.

Consistently, in the immunofluorescence staining (Figure 6f), the significantly higher CD3^+ cell counts (stain green), indicating severer lymphocyte infiltrations, were accumulated at the wound site at day 6 after incision, in controls than in the hydrogel-treated rats. And slight macrophage (CD68 , stain red) invasion into the wound site in both groups was observed. These results indicated the inflammatory response in the control group was much severe as compared with the hydrogel group, after 6 days treatment.

CONCLUSION

In summary, we developed a hydrogel for wound healing with high adhesiveness, toughness, and cell affinity. Unlike those antibacterial hydrogels developed before, the present hydrogel demonstrated excellent contact-active antibacterial properties. CATNFC was applied in hydrogels to render wide-spectrum antibacterial activities and improve their mechanical properties. Owing to the strong crosslinked network and the presence of dynamic noncovalent bonds, the DN hydrogel exhibited desirable mechanical properties and self-healing abilities. Besides, the as-prepared hydrogel could be easily recycled without any pollution. The antibacterial test in vitro, cell affinity and wound healing experiments consistently indicated that the hydrogel could be used as an all-rounded biomaterial in preventing bacterial infection

and promoting tissue regeneration. Given these outstanding properties, the present hydrogel was envisaged to have high potential in skin wound repair.

EXPERIMENTAL SECTION

Materials:

Methanol, ether, sodium hydroxide (NaOH), ammonium persulfate (APS), epichlorohydrin, isopropanol, sodium dihydrogen phosphate (NaH₂PO₄), dipotassium phosphate (K₂HPO₄), aluminum chloride hydrate (AlCl₃· 2O), acrylic acid (AAc) and acrylamide (AM) were supplied by Kelong Co., Ltd. (Chengdu, China). Epoxypropyl trimethylammonium chloride (EPTMAC), N, N-dimethyl dodecyl amine (DDA), dopamine hydrochloride (DA), N-Hydroxysuccinimide (NHS), sodium alginate (Alg) and N-(3-Dimethylaminopropyl)-N'-ethylcarbodiimide hydrochloride (EDC) were purchased from Aladdin Co. (Shanghai, China). Never-dried bamboo pulp was supplied by Yongfeng Paper Co., Ltd. (Muchuan, China). Deuterated chloroform (CDCl₃) and deuterium oxide (D₂O) were supplied by Chengxi High-Tech Incubator Co., Ltd. (Beijing, China). Dulbecco's Modified Eagle Medium (DMEM) and fetal bovine serum (FBS) were purchased from Gibco (Carlsbad, CA, USA).

Preparation of Epoxypropyl Dodecyl Dimethyl Ammonium Chloride (EPDDMAC):

Methanol (5 mL) and N, N-dimethyl dodecyl amine (9.68 g) were placed in a three-necked round bottom flask (100 mL). Next, methanol (5 mL) and epichlorohydrin (4.84 g) were added dropwise to the three-necked round bottom flask. The mixed liquid was maintained at 45 °C for 2 h under the protection of nitrogen. The methanol was then removed via rotary distillation. The product was washed five times with ether and dried at 40 °C for 24 h.

Preparation of cationized nanofibrillated cellulose (CATNFC) dispersions:

80 g never-dried bamboo pulp was dispersed in 2000 mL distilled water, then the suspension was treated using an ultra-fine friction grinder Supermass Colloider (MKCA6-2, Masuko Sangyo Co., Ltd., Japan) at 1500 rpm to make the nanofibrillated cellulose (NFC) dispersion.

And the NFC isopropanol dispersion was prepared by the solvent exchange method. EPDDMAC and NaOH were added to the NFC isopropanol dispersion (1%, w/w) and reacted at 45 °C for 3 h. Finally, the aqueous dispersions of CATNFC were obtained by solvent exchange. In order to synthesize products with different degree of substitution (DS), different raw material ratios were adopted as listed in Table S1.

Graft EPTMAC to NFC (EPTMAC-NFC):

EPTMAC and NaOH (Table S1) were added to the NFC isopropanol dispersion (1%, w/w) and reacted at 45 °C for 3 h. And the aqueous dispersions of EPTMAC-NFC were obtained by solvent exchange.

Synthesis of alginate-dopamine (Alg-DA):

The alginate (3g) was dissolved in 300 mL deionized water at a pH of 5.5. When the alginate was completely dissolved, EDC (5.82 g) and NHS (6.96 g) were added and stirred for 30 min. After that, DA (5.76 g) was added to the reaction solution, and further stirred for 24 h under a nitrogen atmosphere. A dialysis membrane (14000 Da) was used to purify Alg-DA in deionized water for 3 days. Finally, Alg-DA powder was obtained by freeze-drying.

Preparation of DN hydrogels:

The preparation of the DN hydrogel was conducted in two steps. Firstly, the single-network hydrogel was prepared by in-situ radical polymerization. Secondly, it was subjected to metal-ligand coordination crosslinking to form a DN hydrogel. Hydrogels were prepared in the solution containing AM (5.5 g), Alg-DA (0.3 g), AAc (0.279 g, 5mol% of AM), APS (30 mg) and CATNFC ($DS=0.182$) dispersion (10 g, 1 wt%). After 15 min of sonication, the solution was removed into a mold with an internal diameter of 10 mm, and then placed at 60 °C for 4 h to develop the Alg-DA-CATNFC-PAM hydrogel. Next, the prepared hydrogel was immersed in aluminum ion solutions with a given concentration (0.7 M, 0.9 M, 0.11 M, 0.13 M, and 0.15 M) for the metal coordination cross-linking to form a DN hydrogel.

Characterization of EPDDMAC:

DDA and EPDDMAC were examined by a Fourier transform infrared (FTIR) spectrometer (Nicolet Magna-IR 550, USA). The chemical structures of DDA and EPDDMAC were analyzed by a proton nuclear magnetic resonance (^1H NMR) spectrometer (AV III HD 400 MHz, Bruker, USA), with deuterated chloroform (CDCl_3) as the solvent.

Characterization of CATNFC:

The attenuated total reflectance (ATR) infrared spectra for NFC and CATNFC were obtained by a Fourier transform infrared (FTIR) spectrometer (Nicolet Magna-IR 550, USA). Their elemental composition was measured with an elemental analyzer (Euro Vector EA3000, Italy). To convert the mass fraction to mole fraction, it is assumed that each nitrogen atom in the quaternate sample contains one chlorine atom. Hence, the number per anhydroglucose unit (AGU) was estimated according to the following equation (1).

$$DS = \frac{162 \times W_N}{14 - 306.5 \times W_N} \quad (1)$$

162 is the molar mass of AGU of cellulose.

306.5 is the molar mass for each substituted etherifying agent.

14 is the molar mass of nitrogen.

W_N is the mass fraction of nitrogen.

The quantitative assessment of the antibacterial activity against *Escherichia coli* (*E. Coli*, ATCC 8739) was carried out according to the ATCC Test Method 100. The bacteria were revived via growth in a nutrient broth for 16 h. NFC and EPTMAC-NFC ($DS=0.192$) were used as reference along with the CATNFC ($DS=0.182$) sample. Then aliquots of 100 μL inoculum were inoculated for each membrane sample (modified and unmodified) at least twice. After 24 h incubation at 37 $^\circ\text{C}$, 50 mL of the neutralization solution was used to extract the bacteria. Finally, the neutralization solution collected from each membrane was spread on the

counting plate.

Characterization of alginate-dopamine (Alg-DA):

The spectrophotometer UV-1800 (Mapada Instruments Co, China) and the proton nuclear magnetic resonance (^1H NMR) spectrometer (AV III HD 400 MHz, Bruker, USA) were used to characterize the as-synthesized Alg-DA. Deuterium oxide (D_2O) was used as the solvent.

Characterization of DN hydrogels:

The field emission scanning electron microscope (JSM-7500F, Japan) was used to observe the micro morphology of freeze-dried hydrogels. And the corresponding EDS elemental mapping (for elements C, O, N, Cl and Al, as indicated) was obtained at the surface of the freeze-dried hydrogel.

Mechanical property testing:

Cylindrical hydrogel specimens ($D = 15$ mm, $H = 15$ mm) were molded for compression testing, while rectangular specimens ($L = 10$ mm, $W = 20$ mm) were used for tensile testing. The mechanical properties of the hydrogels were measured on a universal testing machine (5567, Instron, USA) with a 100 N load cell. A speed of 2 mm min^{-1} was used in the compressive test, while 5 mm min^{-1} was applied in the tensile test.

In vitro antibacterial activity:

To analyze the antibacterial activities, *S. aureus* (ATCC 29213, gram-positive bacteria) and *E. Coli*. (ATCC 8739, gram-negative bacteria) were used. The hydrogel with Al^{3+} and CATNFC was tested, while the hydrogels without Al^{3+} and CATNFC were used as a control. The antibacterial activities of four hydrogels (30 μg for each one): Alg-DA-PAM, Alg-DA-PAM- Al^{3+} , Alg-DA-CATNFC-PAM and the Alg-DA-CATNFC-PAM- Al^{3+} (0.11M) hydrogels were quantified according to the inhibited rates against *S. aureus* and *E. coli*. Here, aliquots of 100 μL bacteria suspensions (1×10^6 CFU/mL) were incubated with different hydrogels for 4 h. 900 μL of LB broth was added into the previous mixture and incubated for 12 h (37 $^\circ\text{C}$, 120

rpm). Subsequently, 200 μ L of bacteria suspensions were sampled. The optical density (OD) of bacteria suspensions were quantified at 600 nm by micro plate reader (MQX200). The bactericidal ratios (%) of different hydrogels were evaluated according to the following equation.

$$\text{Bactericidal ratio (\%)} = \frac{\text{OD of contrastive groups} - \text{OD of external groups}}{\text{OD of contrastive groups}} \times 100\% \quad (2)$$

In Vitro Cell Affinity:

L929 fibroblast cells were harvested by trypsin. The cells were suspended in the culture medium. Before cell seeding, Alg-DA-PAM, Alg-DA-PAM-Al³⁺, Alg-DA-CATNFC-PAM and the Alg-DA-CATNFC-PAM-Al³⁺ (0.11M) hydrogels (8 mm in diameter, 2.5 mm in thickness) were firstly purified using phosphate buffer solution (PBS). The cells were seeded (1×10^5 cells/mL) in each 24-well plate well containing hydrogel, and incubated for 3 h for attachment. Subsequently, 1 mL of DMEM (10% FBS) was added into each well. Cells were further incubated for 24 h. Cell morphology was described under microscope. The viability of cells grown on hydrogels was analyzed by the 3-[4,5-dimethylthiazol-2-yl]-2,5-diphenyl tetrazolium bromide (MTT) assay. After 2- and 5-days of culture, 200 μ L MTT solution was added into every well, and further incubated for 4 h (37 °C). Cell medium was removed after the incubation, leaving the remaining formazan components. 400 μ L of dimethyl sulfoxide (DMSO) were added to dissolve formazan. The absorbance of formazan solutions was quantified at 570 nm.

Healing Infected Skin Incision In Vivo:

Male Sprague-Dawley (SD) rats weighed between 180 to 220 g were used. Infected skin incision was carried out on the back of each rat. Rats were anesthetized using pentobarbital (2 % dissolved in sterile saline, 2 mL/kg), and depilated at the sites of incision. A scalpel was used to cut a 30 mm opening on the back skin of the experimental rats and bacterial liquid was dripped into the opening. In the hydrogel group, the wound was covered by hydrogel of Alg-

DA-CATNFC-PAM- Al^{3+} (0.11M), while the control group was treated with hemostasis only. After 6 days post-surgery, the rats were sacrificed, and the skins ($2 \times 4 \text{ cm}^2$) were collected for histological analyses. The wound closure rate was calculated using the following equation (3):

$$\text{Wound closure rate} = \frac{L_{\text{initial}} - L_{\text{current}}}{L_{\text{initial}}} \times 100\% \quad (3)$$

Where L_{initial} represented the initial length of the wounds, and L_{current} represented the current length of wounds. For each test, there were three replicates.

ASSOCIATED CONTENT

Supporting Information

Preparation process of Alg-DA, FTIR and ^1H NMR analysis of EPDDMAC, FTIR analysis and antibacterial test of CATNFC, ^1H NMR and UV - Vis analysis of Alg-DA, SEM, EDS and cell affinity analysis of DN hydrogel, and the table listing ratios of raw materials for the synthesis of CATNFC.

AUTHOR INFORMATION

Author Contributions

‡These authors contributed equally.

Notes

The authors declare no competing financial interest.

ACKNOWLEDGMENT

This work was supported by the National Natural Science Foundation of China (32070826 and 51861165203), the Chinese Postdoctoral Science Foundation (2019M650239, 2020T130762), the Sichuan Science and Technology Program (2019YJ0125), the State Key Laboratory of Polymer Materials Engineering (sklpme2019-2-19), the Chongqing Research Program of Basic Research and Frontier Technology (cstc2018jcyjAX0807), the Science and

Technology Committee of Yubei District [2019(GY)07] and the RCUK China-UK Science Bridges Program through the Medical Research Council, and the Fundamental Research Funds for the Central Universities.

REFERENCES

- (1) Pazyar, N.; Yaghoobi, R.; Rafiee, E.; Mehrabian, A.; Feily, A. Skin Wound Healing and Phytomedicine: A Review. *Skin Pharmacol. Physiol.* **2014**, *27* (6), 303–310.

DOI: 10.1159/000357477
- (2) Xu, R.; Luo, G.; Xia, H.; He, W.; Zhao, J.; Liu, B.; Tan, J.; Zhou, J.; Liu, D.; Wang, Y.; Yao, Z.; Zhan, R.; Yang, S.; Wu, J. Novel Bilayer Wound Dressing Composed of Silicone Rubber with Particular Micropores Enhanced Wound Re-Epithelialization and Contraction. *Biomaterials* **2015**, *40*, 1–11.

DOI: 10.1016/j.biomaterials.2014.10.077
- (3) Gong, C. Y.; Wu, Q. J.; Wang, Y. J.; Zhang, D. D.; Luo, F.; Zhao, X.; Wei, Y. Q.; Qian, Z. Y. A Biodegradable Hydrogel System Containing Curcumin Encapsulated in Micelles for Cutaneous Wound Healing. *Biomaterials* **2013**, *34* (27), 6377–6387.

DOI: 10.1016/j.biomaterials.2013.05.005
- (4) Deng, J.; Tang, Y.; Zhang, Q.; Wang, C.; Liao, M.; Ji, P.; Song, J.; Luo, G.; Chen, L.; Ran, X.; Wei, Z.; Zheng, L.; Dang, R.; Liu, X.; Zhang, H.; Zhang, Y. S.; Zhang, X.; Tan, H. A Bioinspired Medical Adhesive Derived from Skin Secretion of *Andrias Davidianus* for Wound Healing. *Adv. Funct. Mater.* **2019**, *29* (31), 1–13.

DOI: 10.1002/adfm.201809110
- (5) Nudelman, R.; Alhmoud, H.; Delalat, B.; Fleicher, S.; Fine, E.; Guliakhmedova, T.;

Elnathan, R.; Nyska, A.; Voelcker, N. H.; Gozin, M.; Richter, S. Jellyfish-Based Smart Wound Dressing Devices Containing In Situ Synthesized Antibacterial Nanoparticles. *Adv. Funct. Mater.* **2019**, *29* (38), 1–11.

DOI: 10.1002/adfm.201902783

- (6) Tran, P. L.; Hamood, A. N.; De Souza, A.; Schultz, G.; Liesenfeld, B.; Mehta, D.; Reid, T. W. A Study on the Ability of Quaternary Ammonium Groups Attached to a Polyurethane Foam Wound Dressing to Inhibit Bacterial Attachment and Biofilm Formation. *Wound Repair Regen.* **2015**, *23* (1), 74–81.

DOI: 10.1111/wrr.12244

- (7) Li, J.; Zhai, D.; Lv, F.; Yu, Q.; Ma, H.; Yin, J.; Yi, Z.; Liu, M.; Chang, J.; Wu, C. Preparation of Copper-Containing Bioactive Glass/Eggshell Membrane Nanocomposites for Improving Angiogenesis, Antibacterial Activity and Wound Healing. *Acta Biomater.* **2016**, *36*, 254–266.

DOI: 10.1016/j.actbio.2016.03.011

- (8) Liu, B.; Wang, Y.; Miao, Y.; Zhang, X.; Fan, Z.; Singh, G.; Zhang, X.; Xu, K.; Li, B.; Hu, Z.; Xing, M. Hydrogen Bonds Autonomously Powered Gelatin Methacrylate Hydrogels with Super-Elasticity, Self-Heal and Underwater Self-Adhesion for Sutureless Skin and Stomach Surgery and E-Skin. *Biomaterials* **2018**, *171*, 83–96.

DOI: 10.1016/j.biomaterials.2018.04.023

- (9) Dong, Y.; Hassan, W. U.; Kennedy, R.; Greiser, U.; Pandit, A.; Garcia, Y.; Wang, W. Performance of an in Situ Formed Bioactive Hydrogel Dressing from a PEG-Based

- Hyperbranched Multifunctional Copolymer. *Acta Biomater.* **2014**, *10* (5), 2076–2085.
- DOI: 10.1016/j.actbio.2013.12.045
- (10) Zhou, L.; Xi, Y.; Xue, Y.; Wang, M.; Liu, Y.; Guo, Y.; Lei, B. Injectable Self-Healing Antibacterial Bioactive Polypeptide-Based Hybrid Nanosystems for Efficiently Treating Multidrug Resistant Infection, Skin-Tumor Therapy, and Enhancing Wound Healing. *Adv. Funct. Mater.* **2019**, *29* (22), 1–11.
- DOI: 10.1002/adfm.201806883
- (11) Blacklow, S. O.; Li, J.; Freedman, B. R.; Zeidi, M.; Chen, C.; Mooney, D. J. Bioinspired Mechanically Active Adhesive Dressings to Accelerate Wound Closure. *Sci. Adv.* **2019**, *5* (7), 1–10.
- DOI: 10.1126/sciadv.aaw3963
- (12) Qu, J.; Zhao, X.; Liang, Y.; Zhang, T.; Ma, P. X.; Guo, B. Antibacterial Adhesive Injectable Hydrogels with Rapid Self-Healing, Extensibility and Compressibility as Wound Dressing for Joints Skin Wound Healing. *Biomaterials* **2018**, *183*, 185–199.
- DOI: 10.1016/j.biomaterials.2018.08.044
- (13) Zhao, X.; Wu, H.; Guo, B.; Dong, R.; Qiu, Y.; Ma, P. X. Antibacterial Anti-Oxidant Electroactive Injectable Hydrogel as Self-Healing Wound Dressing with Hemostasis and Adhesiveness for Cutaneous Wound Healing. *Biomaterials* **2017**, *122*, 34–47.
- DOI: 10.1016/j.biomaterials.2017.01.011
- (14) Fu, L. H.; Qi, C.; Ma, M. G.; Wan, P. Multifunctional Cellulose-Based Hydrogels for

- Biomedical Applications. *J. Mater. Chem. B* **2019**, 7 (10), 1541–1562.
- DOI: 10.1039/c8tb02331j
- (15) Saini, S.; Belgacem, N.; Mendes, J.; Elegir, G.; Bras, J. Contact Antimicrobial Surface Obtained by Chemical Grafting of Microfibrillated Cellulose in Aqueous Solution Limiting Antibiotic Release. *ACS Appl. Mater. Interfaces* **2015**, 7 (32), 18076–18085.
- DOI: 10.1021/acsami.5b04938
- (16) Jain, A.; Duvvuri, L. S.; Farah, S.; Beyth, N.; Domb, A. J.; Khan, W. Antimicrobial Polymers. *Adv. Healthc. Mater.* **2014**, 3 (12), 1969–1985.
- DOI: 10.1002/adhm.201400418
- (17) Ikeda, T.; Hirayama, H.; Yamaguchi, H.; Tazuke, S.; Watanabe, M. Polycationic Biocides with Pendant Active Groups: Molecular Weight Dependence of Antibacterial Activity. *Antimicrob. Agents Chemother.* **1986**, 30 (1), 132–136.
- DOI: 10.1128/AAC.30.1.132
- (18) He, J.; Söderling, E.; Vallittu, P. K.; Lassila, L. V. J. Investigation of Double Bond Conversion, Mechanical Properties, and Antibacterial Activity of Dental Resins with Different Alkyl Chain Length Quaternary Ammonium Methacrylate Monomers (QAM). *J. Biomater. Sci. Polym. Ed.* **2013**, 24 (5), 565–573.
- DOI: 10.1080/09205063.2012.699709
- (19) Rauner, N.; Meuris, M.; Zoric, M.; Tiller, J. C. Enzymatic Mineralization Generates Ultrastiff and Tough Hydrogels with Tunable Mechanics. *Nature* **2017**, 543 (7645), 407–410.

DOI: 10.1038/nature21392

- (20) Chen, H.; Liu, Y.; Ren, B.; Zhang, Y.; Ma, J.; Xu, L.; Chen, Q.; Zheng, J. Super Bulk and Interfacial Toughness of Physically Crosslinked Double-Network Hydrogels. *Adv. Funct. Mater.* **2017**, *27* (44), 1–10.

DOI: 10.1002/adfm.201703086

- (21) Wang, L.; Zhang, X.; Xia, Y.; Zhao, X.; Xue, Z.; Sui, K.; Dong, X.; Wang, D. Cooking-Inspired Versatile Design of an Ultrastrong and Tough Polysaccharide Hydrogel through Programmed Supramolecular Interactions. *Adv. Mater.* **2019**, *31* (41), 1–8.

DOI: 10.1002/adma.201902381

- (22) Sun, J. Y.; Zhao, X.; Illeperuma, W. R. K.; Chaudhuri, O.; Oh, K. H.; Mooney, D. J.; Vlassak, J. J.; Suo, Z. Highly Stretchable and Tough Hydrogels. *Nature* **2012**, *489* (7414), 133–136.

DOI: 10.1038/nature11409

- (23) Zhao, X.; Liang, Y.; Huang, Y.; He, J.; Han, Y.; Guo, B. Physical Double-Network Hydrogel Adhesives with Rapid Shape Adaptability, Fast Self-Healing, Antioxidant and NIR/PH Stimulus-Responsiveness for Multidrug-Resistant Bacterial Infection and Removable Wound Dressing. *Adv. Funct. Mater.* **2020**, *30* (17), 1–18.

DOI: 10.1002/adfm.201910748

- (24) Wang, X. H.; Song, F.; Qian, D.; He, Y. D.; Nie, W. C.; Wang, X. L.; Wang, Y. Z. Strong and Tough Fully Physically Crosslinked Double Network Hydrogels with Tunable Mechanics and High Self-Healing Performance. *Chem. Eng. J.* **2018**, *349* (May), 588–594.

DOI: 10.1016/j.cej.2018.05.081

- (25) Deng, Z.; Guo, Y.; Zhao, X.; Ma, P. X.; Guo, B. Multifunctional Stimuli-Responsive Hydrogels with Self-Healing, High Conductivity, and Rapid Recovery through Host-Guest Interactions. *Chem. Mater.* **2018**, *30* (5), 1729–1742.

DOI: 10.1021/acs.chemmater.8b00008

- (26) Wei, Z.; Yang, J. H.; Liu, Z. Q.; Xu, F.; Zhou, J. X.; Zrínyi, M.; Osada, Y.; Chen, Y. M. Novel Biocompatible Polysaccharide-Based Self-Healing Hydrogel. *Adv. Funct. Mater.* **2015**, *25* (9), 1352–1359.

DOI: 10.1002/adfm.201401502

- (27) Yan, B.; Huang, J.; Han, L.; Gong, L.; Li, L.; Israelachvili, J. N.; Zeng, H. Duplicating Dynamic Strain-Stiffening Behavior and Nanomechanics of Biological Tissues in a Synthetic Self-Healing Flexible Network Hydrogel. *ACS Nano* **2017**, *11* (11), 11074–11081.

DOI: 10.1021/acsnano.7b05109

- (28) Wang, P.; Deng, G.; Zhou, L.; Li, Z.; Chen, Y. Ultrastretchable, Self-Healable Hydrogels Based on Dynamic Covalent Bonding and Triblock Copolymer Micellization. *ACS Macro Lett.* **2017**, *6* (8), 881–886.

DOI: 10.1021/acsmacrolett.7b00519

- (29) Liang, Y.; Zhao, X.; Hu, T.; Chen, B.; Yin, Z.; Ma, P. X.; Guo, B. Adhesive Hemostatic Conducting Injectable Composite Hydrogels with Sustained Drug Release and

Photothermal Antibacterial Activity to Promote Full-Thickness Skin Regeneration During Wound Healing. *Small* **2019**, *15* (12), 1–17.

DOI: 10.1002/sml.201900046

- (30) Tang, P.; Han, L.; Li, P.; Jia, Z.; Wang, K.; Zhang, H.; Tan, H.; Guo, T.; Lu, X. Mussel-Inspired Electroactive and Antioxidative Scaffolds with Incorporation of Polydopamine-Reduced Graphene Oxide for Enhancing Skin Wound Healing. *ACS Appl. Mater. Interfaces* **2019**, *11* (8), 7703–7714.

DOI: 10.1021/acsami.8b18931

- (31) Gan, D.; Xing, W.; Jiang, L.; Fang, J.; Zhao, C.; Ren, F.; Fang, L.; Wang, K.; Lu, X. Plant-Inspired Adhesive and Tough Hydrogel Based on Ag-Lignin Nanoparticles Triggered Dynamic Redox Catechol Chemistry. *Nat. Commun.* **2019**, *10* (1), 1–10.

DOI: 10.1038/s41467-019-09351-2

- (32) Zhao, Q.; Lee, D. W.; Ahn, B. K.; Seo, S.; Kaufman, Y.; Israelachvili, J. N.; Waite, J. H. Underwater Contact Adhesion and Microarchitecture in Polyelectrolyte Complexes Actuated by Solvent Exchange. *Nat. Mater.* **2016**, *15* (4), 407–412.

DOI: 10.1038/nmat4539

- (33) Liang, Y.; Zhao, X.; Hu, T.; Han, Y.; Guo, B. Mussel-Inspired, Antibacterial, Conductive, Antioxidant, Injectable Composite Hydrogel Wound Dressing to Promote the Regeneration of Infected Skin. *J. Colloid Interface Sci.* **2019**, *556*, 514–528.

DOI: 10.1016/j.jcis.2019.08.083

- (34) Liang, Y.; Chen, B.; Li, M.; He, J.; Yin, Z.; Guo, B. Injectable Antimicrobial Conductive Hydrogels for Wound Disinfection and Infectious Wound Healing. *Biomacromolecules* **2020**, *21*(5), 1841–1852.
- DOI: 10.1021/acs.biomac.9b01732
- (35) Kim, B. J.; Oh, D. X.; Kim, S.; Seo, J. H.; Hwang, D. S.; Masic, A.; Han, D. K.; Cha, H. J. Mussel-Mimetic Protein-Based Adhesive Hydrogel. *Biomacromolecules* **2014**, *15*(5), 1579–1585.
- DOI: 10.1021/bm4017308
- (36) Gan, D.; Xu, T.; Xing, W.; Ge, X.; Fang, L.; Wang, K.; Ren, F.; Lu, X. Mussel Inspired Contact-Active Antibacterial Hydrogel with High Cell Affinity, Toughness, and Recoverability. *Adv. Funct. Mater.* **2019**, *29* (1), 1–11.
- DOI: 10.1002/adfm.201805964
- (37) Wang, K.; Nune, K. C.; Misra, R. D. K. The Functional Response of Alginate-Gelatin Nanocrystalline Cellulose Injectable Hydrogels toward Delivery of Cells and Bioactive Molecules. *Acta Biomater.* **2016**, *36*, 143–151.
- DOI: 10.1016/j.actbio.2016.03.016
- (38) Li, Y.; Han, Y.; Wang, X.; Peng, J.; Xu, Y.; Chang, J. Multifunctional Hydrogels Prepared by Dual Ion Cross-Linking for Chronic Wound Healing. *ACS Appl. Mater. Interfaces* **2017**, *9* (19), 16054–16062.
- DOI: 10.1021/acsami.7b04801

- (39) Suárez-González, D.; Barnhart, K.; Saito, E.; Vanderby, R.; Hollister, S. J.; Murphy, W. L. Controlled Nucleation of Hydroxyapatite on Alginate Scaffolds for Stem CellBased Bone Tissue Engineering. *J. Biomed. Mater. Res. - Part A* **2010**, *95* (1), 222–234.
DOI: 10.1002/jbm.a.32833
- (40) Zhang, S.; Xu, K.; Darabi, M. A.; Yuan, Q.; Xing, M. Mussel-Inspired Alginate Gel Promoting the Osteogenic Differentiation of Mesenchymal Stem Cells and Anti-Infection. *Mater. Sci. Eng. C* **2016**, *69*, 496–504.
DOI: 10.1016/j.msec.2016.06.044
- (41) Han, L.; Lu, X.; Liu, K.; Wang, K.; Fang, L.; Weng, L. T.; Zhang, H.; Tang, Y.; Ren, F.; Zhao, C.; Sun, G.; Liang, R.; Li, Z. Mussel-Inspired Adhesive and Tough Hydrogel Based on Nanoclay Confined Dopamine Polymerization. *ACS Nano* **2017**, *11* (3), 2561–2574.
DOI: 10.1021/acsnano.6b05318
- (42) Liu, Y.; Chen, Y.; Zhao, Y.; Tong, Z.; Chen, S. Superabsorbent Sponge and Membrane Prepared by Polyelectrolyte Complexation of Carboxymethyl Cellulose/Hydroxyethyl Cellulose- Al^{3+} . *BioResources*. **2015**, *10* (4), 6479–6495.
DOI: 10.15376/biores.10.4.6479-6495
- (43) Wang, W.; Zhang, Y.; Liu, W. Bioinspired Fabrication of High Strength Hydrogels from Non-Covalent Interactions. *Prog. Polym. Sci.* **2017**, *71*, 1–25.
DOI: 10.1016/j.progpolymsci.2017.04.001
- (44) Londono, S. C.; Hartnett, H. E.; Williams, L. B. Antibacterial Activity of Aluminum in Clay from the Colombian Amazon. *Environ. Sci. Technol.* **2017**, *51* (4), 2401–2408.

DOI: 10.1021/acs.est.6b04670

- (45) Welage, L.; Carver, P.; Welch, K. Antibacterial Activity of Sucralfate versus Aluminum Chloride in Simulated Gastric Fluid. *Eur. J. Clin. Microbiol. Infect. Dis.* **1994**, *13* (12), 1046–1052.

DOI: 10.1007/BF02111825

- (46) Addisu, K. D.; Hailemeskel, B. Z.; Mekuria, S. L.; Andrgie, A. T.; Lin, Y. C.; Tsai, H. C. Bioinspired, Manganese-Chelated Alginate-Polydopamine Nanomaterials for Efficient in Vivo T1-Weighted Magnetic Resonance Imaging. *ACS Appl. Mater. Interfaces.* **2018**, *10* (6), 5147-5160.

DOI: 10.1021/acsami.7b13396

- (47) Shao, C.; Chang, H.; Wang, M.; Xu, F.; Yang, J. High-Strength, Tough, and Self-Healing Nanocomposite Physical Hydrogels Based on the Synergistic Effects of Dynamic Hydrogen Bond and Dual Coordination Bonds. *ACS Appl. Mater. Interfaces* **2017**, *9* (34), 28305–28318.

DOI: 10.1021/acsami.7b09614

- (48) Zeng, H.; Soo, D.; Israelachvili, J. N.; Waite, J. H. Strong Reversible Fe³⁺-Mediated Bridging between Dopa-Containing Protein Films in Water. *Proc. Natl. Acad. Sci. U. S. A.* **2010**, *107* (29) 10–13.

DOI: 10.1073/pnas.1007416107

- (49) Holten-Andersen, N.; Harrington, M. J.; Birkedal, H.; Lee, B. P.; Messersmith, P. B.; Lee, K. Y. C.; Waite, J. H. PH-Induced Metal-Ligand Cross-Links Inspired by Mussel Yield Self-Healing Polymer Networks with near-Covalent Elastic Moduli. *Proc. Natl.*

Acad. Sci. U. S. A. **2011**, *108* (7), 2651–2655.

DOI: 10.1073/pnas.1015862108

- (50) Gao, L.; Zhou, Y.; Peng, J.; Xu, C.; Xu, Q.; Xing, M.; Chang, J. A Novel Dual Adhesive and Bioactive Hydrogel Activated by Bioglass for Wound Healing. *NPG Asia Mater.* **2019**, *11* (1), 1-11.

DOI: 10.1038/s41427-019-0168-0

- (51) Desjardins-Park, H. E.; Foster, D. S.; Longaker, M. T. Fibroblasts and Wound Healing: An Update. *Regen. Med.* **2018**, *13* (5), 491–495.

DOI: 10.2217/rme-2018-0073

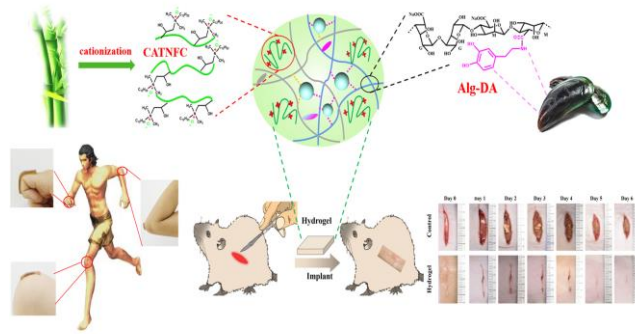
- (52) Yao, X. -L.; Jenkins, E. C.; Wisniewski, H. M. Effect of Aluminum Chloride on Mitogenesis, Mitosis, and Cell Cycle in Human Short-term Whole Blood Cultures: Lower Concentrations Enhance Mitosis. *J. Cell. Biochem.* **1994**, *54* (4), 473–477.

DOI: 10.1002/jcb.240540414

- (53) Dominguez, M. C.; Sole, E.; Goñi, C.; Ballabriga, A. Effect of Aluminum and Lead Salts on Lipid Peroxidation and Cell Survival in Human Skin Fibroblasts. *Biol. Trace Elem. Res.* **1995**, *47* (1–3)

DOI: 10.1007/BF02790101

TOC:



Antibacterial hydrogels with excellent adhesiveness were prepared from renewable and sustainable biopolymers (cellulose and alginate) for effective wound healing.